Dirac quantum walks on triangular and honeycomb lattices

Gareth Jay,[1,*] Fabrice Debbasch,[2,†] and J. B. Wang[1,‡]
[1]*Physics Department, The University of Western Australia, Perth, Western Australia 6009, Australia*
[2]*Sorbonne Université, Observatoire de Paris, Université PSL, CNRS, LERMA, F-75005, Paris, France*

(Received 11 March 2018; published 14 March 2019)

In this paper, we present a detailed study on discrete-time Dirac quantum walks (DQWs) on triangular and honeycomb lattices. At the continuous limit, these DQWs coincide with the Dirac equation. Their differences in the discrete regime are analyzed through the dispersion relations, with special emphasis on Zitterbewegung. An extension which couples these walks to arbitrary discrete electromagnetic field is also proposed and the resulting Bloch-like oscillations are discussed.

DOI: 10.1103/PhysRevA.99.032113

I. INTRODUCTION

Quantum walks were first considered by Feynman in studying possible discretizations for the Dirac path integral [1,2]. They were later introduced in a systematic way by Aharonov *et al.* [3] and Meyer [4]. Quantum walks are simple models of coherent quantum transport on discrete structures such as graphs and lattices. They have attracted a lot of attention in quantum information and algorithmic development [5–7]. They can also be used as quantum simulators [8–16], with the lattice now representing a discretization of continuous space. On the other hand, in a more adventurous way, quantum walks may represent a potentially realistic discrete space underlying the apparently continuous physical universe [17].

It has been shown recently that several discrete-time quantum walks defined on regular square lattices simulate the Dirac dynamics in various space-time dimensions and that these walks (termed as DQWs) can be coupled to various discrete gauge fields [18–24]. In particular, some DQWs can be coupled to discrete electric and magnetic fields in a gauge-invariant manner [19–21,25], and magnetic confinement as well as Bloch oscillations have been observed. To the best of our knowledge the only DQW which has been defined on a nonsquare lattice [26] has not been coupled to gauge fields. A natural, yet unanswered question is therefore: Can DQWs defined on square lattices be coupled to gauge fields and, if so, which aspects of the dynamics depend on the choice of lattice, and which do not? The present paper is a step in answering this question.

We focus on the transport properties of quantum walks in $(1+2)D$ space-time dimensions and propose four new unitary DQWs defined on triangular and honeycomb lattices. Two of these DQWs are defined on the same lattice made out of equilateral triangles, the third DQW is defined on a lattice of isosceles triangles, and the last is on a hexagonal honeycomb lattice. At the continuous limit, all four walks are equivalent and coincide with the free Dirac equation. However, the walks greatly differ outside this limit and the differences are analyzed through the dispersion relations [27–29], with special emphasis on Zitterbewegung [30–32]. We also discuss how these walks can be extended to include a gauge-invariant coupling to arbitrary electromagnetic fields. The extension is built in full for the simplest walk defined on the equilateral triangle lattice, for which Bloch-like oscillations [33,34] are also addressed. These results show that DQWs defined on more general lattices than the square lattice can be used to study the free Dirac dynamics and that coupling the walks to arbitrary electromagnetic fields in a gauge-invariant manner is also possible.

II. FOUR FREE QUANTUM WALKS ON NONSQUARE LATTICES

A. Six-step walk on the equilateral triangular lattice

Let (x, y) be orthonormal coordinates on the plane and focus first on the regular lattice made of equilateral triangles of side ϵ. Choose one site S at position $\mathbf{X} = (x, y)$ and let its six neighbors $N_j(\mathbf{X})$ have the respective coordinates

$$\begin{aligned} N_1(\mathbf{X}) &= (x+\epsilon, y),\\ N_2(\mathbf{X}) &= (x+\epsilon/2, y+\sqrt{3}\epsilon/2),\\ N_3(\mathbf{X}) &= (x-\epsilon/2, y+\sqrt{3}\epsilon/2),\\ N_4(\mathbf{X}) &= (x-\epsilon, y),\\ N_5(\mathbf{X}) &= (x-\epsilon/2, y-\sqrt{3}\epsilon/2),\\ N_6(\mathbf{X}) &= (x+\epsilon/2, y-\sqrt{3}\epsilon/2). \end{aligned} \tag{1}$$

Let $\Psi = (\psi^L, \psi^R)^\top$ be a two-component spinor defined on the lattice and define six translation operators S_j by $(S_j\Psi)(\mathbf{X}) = (\psi^L(N_j(\mathbf{X})), \psi^R(N_{j+1}(\mathbf{X})))^\top$, where $N_7 = N_1$. Consider the DQW defined by $\Psi(t+\Delta t) = W_0\Psi(t)$ with $W_0 = \Pi_{j=6}^{1} W_j = W_6 \ldots W_1$ where

$$\begin{aligned} W_j &= R_j^{-1} U_j S_j R_j,\\ R_j &= U(0, \pi/2, 0, \pi/12 + (j-1)\pi/6),\\ U_j &= U(0,0,0,0) = 1, \end{aligned} \tag{2}$$

*gareth.jay@uwa.edu.au
†fabrice.debbasch@gmail.com
‡jingbo.wang@uwa.edu.au

where an arbitrary element U of $U(2)$ can be parametrized by four angles

$$U(\alpha,\xi,\zeta,\theta)=e^{i\alpha}\begin{pmatrix} e^{i\xi}\cos\theta & e^{i\zeta}\sin\theta \\ -e^{-i\zeta}\sin\theta & e^{-i\xi}\cos\theta\end{pmatrix}. \tag{3}$$

Introducing the operators U_j seems useless because, at this stage, they all coincide with the unit operator. This is so because, as explained in Sec. IV, these operators actually code for an electromagnetic field acting on the walk and we are considering only free walks in the present section. The more general case is described in Sec. IV.

Set now $\Delta t=3\epsilon/2$ and let ϵ tend to zero. The formal limit of this DQW exists and coincides then with the massless Dirac equation $\gamma^\mu\partial_\mu\Psi=0$ with $x^0=t$, $x^1=x$, $x^2=y$, and

$$\gamma^0=\sigma_1=\begin{pmatrix}0&1\\1&0\end{pmatrix},$$
$$\gamma^1=-i\sigma_3=\begin{pmatrix}-i&0\\0&i\end{pmatrix},$$
$$\gamma^2=-i\sigma_2=\begin{pmatrix}0&-1\\1&0\end{pmatrix}. \tag{4}$$

To show this more explicitly, the DQW defined above by $\Psi(t+\Delta t)=W_0\Psi(t)$ gives a difference equation which can be Taylor expanded around $\epsilon=0$. The zeroth-order terms cancel out and the first-order terms give the differential equations

$$\frac{3}{2}\frac{\partial\psi^L}{\partial t}=-\frac{3}{2}\left(i\frac{\partial\psi^R}{\partial x}+\frac{\partial\psi^L}{\partial y}\right),$$
$$\frac{3}{2}\frac{\partial\psi^R}{\partial t}=\frac{3}{2}\left(i\frac{\partial\psi^L}{\partial x}+\frac{\partial\psi^R}{\partial y}\right). \tag{5}$$

This can be rewritten in matrix form as

$$\partial_0\Psi=\begin{pmatrix}0&-i\\i&0\end{pmatrix}\partial_1\Psi+\begin{pmatrix}-1&0\\0&1\end{pmatrix}\partial_2\Psi, \tag{6}$$

from which you can obtain the above Dirac equation simply by multiplying by σ_1. A nonvanishing mass m can be added by replacing W_0 by $W_m=U_mW_0$ with $U_m=U(0,0,-\pi/2,3\epsilon m/2)$.

B. Three-step walk on the equilateral triangular lattice

The walk just presented approximates the Dirac equation in six steps. It is possible to approximate the Dirac equation by a three-step walk defined on the same equilateral lattice. Consider indeed the DQW defined on the same regular triangular lattice by $\Psi(t+\Delta t)=\tilde W_0\Psi(t)$ with $\tilde W_0=\Pi_{j=3}^1\tilde W_j$ where

$$\begin{aligned}\tilde W_j&=\tilde R_{j-1}^{-1}U_j\tilde S_j\tilde R_{j-1},\\ \tilde R_0&=U(0,0,0,0),\\ \tilde R_j&=U(0,\pi/2,0,j\pi/6),\\ (\tilde S_j\Psi)(\mathbf{X})&=(\psi^L(N_j(\mathbf{X})),\psi^R(N_{j+3}(\mathbf{X})))^\top,\end{aligned} \tag{7}$$

and $U_j=U(0,0,0,0)$ as before. This walk with $\Delta t=3\epsilon/2$, and letting ϵ tend to zero has a formal limit that coincides with the same massless Dirac equation as before, except with the gamma matrices this time being

$$\gamma^0=\sigma_1=\begin{pmatrix}0&1\\1&0\end{pmatrix},$$
$$\gamma^1=i\sigma_2=\begin{pmatrix}0&1\\-1&0\end{pmatrix},$$
$$\gamma^2=-i\sigma_3=\begin{pmatrix}-i&0\\0&i\end{pmatrix}. \tag{8}$$

A mass m can be added the same way as the other triangular lattice walk above.

C. Three-step walk on the triangular isosceles lattice

We introduce a closely related walk, which approximates the Dirac equation also in three steps, but is defined on an isosceles triangular lattice. Consider a lattice of isosceles triangles of base ϵ and perpendicular height $\epsilon/2$. Each point $\mathbf{X}=(x,y)$ now has six neighbors defined with the respective coordinates

$$\begin{aligned}N_1(\mathbf{X})&=(x+\epsilon,y),\\ N_2(\mathbf{X})&=(x+\epsilon/2,y+\epsilon/2),\\ N_3(\mathbf{X})&=(x-\epsilon/2,y+\epsilon/2),\\ N_4(\mathbf{X})&=(x-\epsilon,y),\\ N_5(\mathbf{X})&=(x-\epsilon/2,y-\epsilon/2),\\ N_6(\mathbf{X})&=(x+\epsilon/2,y-\epsilon/2).\end{aligned} \tag{9}$$

The corresponding translation operators $\hat S_j$ are defined similar to the three-step walk above. The DQW is then defined as $\Psi(t+\Delta t)=\hat W_0\Psi(t)$ where $\hat W_0=\Pi_{j=3}^1\hat W_j$ with

$$\begin{aligned}\hat W_j&=\hat U_j\hat S_j,\\ \hat U_j&=U(0,0,-\pi/2,(j-2)\pi/4),\\ (\hat S_j\Psi)(\mathbf{X})&=(\psi^L(N_j(\mathbf{X})),\psi^R(N_{j+3}(\mathbf{X})))^\top.\end{aligned} \tag{10}$$

With the choice $\Delta t=\epsilon$, this DQW tends to the Dirac equation with the gamma matrices now being $\gamma^0=\sigma_1$, $\gamma^1=i\sigma_2$, and $\gamma^2=i\sigma_3$. To add a nonvanishing mass m, one can for example replace $\hat U_1$ with $\hat U_m=U(0,0,-\pi/2,-\pi/4+m\epsilon)$.

D. Three-step walk on the honeycomb lattice

We can define DQWs on other lattice structures. For example, let (x,y) be orthonormal coordinates on the plane and consider a regular hexagonal honeycomb lattice of sides ϵ. Choose one site S at position $\mathbf{X}=(x,y)$ and focus on the three neighbors

$$\begin{aligned}N_1(\mathbf{X})&=(x+\epsilon,y),\\ N_2(\mathbf{X})&=(x-\epsilon/2,y+\sqrt{3}\epsilon/2),\\ N_3(\mathbf{X})&=(x-\epsilon/2,y-\sqrt{3}\epsilon/2).\end{aligned} \tag{11}$$

Consider now the DQW defined by $\Psi(t+\Delta t)=W_0\Psi(t)$ with $W_0=\Pi_{j=3}^1W_j$ where

$$\begin{aligned}W_j&=U_j^{-1}S_jU_j,\\ U_j&=U(0,\pi/2,0,\pi/6+(j-1)\pi/3),\\ (S_j\Psi)(\mathbf{X})&=(\psi^L(N_j(\mathbf{X})),\psi^R(N_{j+1}(\mathbf{X})))^\top,\end{aligned} \tag{12}$$

with the convention $N_4(\mathbf{X})=N_1(\mathbf{X})$.

The full honeycomb lattice can be seen as the union of two offset triangular lattices, which we call red and blue for convenience. The above DQW couples sites which are close neighbors on the honeycomb lattice, i.e., at each time step Δt, the quantum states of red sites are translated (and mixed) unto the blue sites and the quantum states of blue sites are translated (and mixed) unto red ones. Note that charge carriers on graphene do indeed transport by jumping between closest neighbors, i.e., between sites of different colors.

Set now $\Delta t = 3\sqrt{3}\epsilon/4$ and let ϵ tend to zero. The formal limit of this DQW exists and coincides then with the massless Dirac equation $\gamma^\mu \partial_\mu \Psi = 0$ with with the gamma matrices $\gamma^0 = \sigma_1$, $\gamma^1 = -i\sigma_3$, and $\gamma^2 = -i\sigma_2$. A mass m can be added to the DQW by replacing W_0 by $W_m = U_m W_0$ with $U_m = U(0, 0, -\pi/2, 3\sqrt{3}\epsilon m/4)$.

E. Equivalence of different choice of gamma matrices and time scaling

The PDEs describing the continuous limit of the various walks considered above are mathematically equivalent because they are simply different representations of the free Dirac equation in flat two-dimensional space-time with gamma matrices obeying the usual Clifford algebra anticommutator relation of $\{\gamma^\mu, \gamma^\nu\} = 2\eta^{\mu\nu}\mathbb{I}$, where $\eta^{\mu\nu}$ is the Minkowski metric. If we consider the first two walks defined above, the first walk uses the set of gamma matrices $\{\sigma_1, -i\sigma_3, -i\sigma_2\}$, while the second walk uses the set $\{\sigma_1, i\sigma_2, -i\sigma_3\}$. If we start with the Dirac equation of the first walk, and then make the coordinate change of $X = -y$ and $Y = x$, we obtain the equation

$$\sigma_1 \partial_t \Psi + i\sigma_2 \partial_X \Psi - i\sigma_3 \partial_Y \Psi, \tag{13}$$

which is the Dirac equation of the second walk. Another coordinate change of $X' = X$ and $Y' = -Y$ will get you to the representation achieved by the third walk, while the continuous limit of fourth walk is delivered in the same representation as the first.

The different scalings of time are simply due to the differences in the space-time lattice that the DQW are operating on. If one looks at the isosceles triangle walk, the lattice could have been regarded as an equilateral triangle lattice but with the DQW taking steps of $\Delta y = \epsilon/\sqrt{3}$ in the y direction compared to steps of $\Delta x = \epsilon$ in the x direction. So if one thinks of that walk as a change in the size of the y dimension, that is creating an isosceles triangle, one can think of the different scalings of Δt as the changing of the height of the three-dimensional triangular (or honeycomb)-based prisms that make up the space-*time* lattice of the walks.

III. DISPERSION RELATIONS AND ZITTERBEWEGUNG

Expanding the discrete equations defining the DQWs furnishes an explicit expression for the value taken by the wave function at time $t + \Delta t$ and point $\mathbf{X}$ in terms of the values taken by the wave function at time t and various neighboring points. These equations can be written in (spatial) Fourier space by introducing

$$\hat{\Psi}(t, \mathbf{k}) = \sum_{\mathbf{X}} \Psi(t, \mathbf{X}) \exp(i\mathbf{k} \cdot \mathbf{X}), \tag{14}$$

where the sum extends to all points of the lattice and $\mathbf{K}$ belongs to the first Brillouin zone. The general form of the equations of motion in Fourier space is

$$\begin{aligned} \hat{\Psi}^L(t + \epsilon, \mathbf{k}) &= E_L^L(\epsilon\mathbf{k})\hat{\Psi}^L(t, \mathbf{k}) + E_R^L(\epsilon\mathbf{k})\hat{\Psi}^R(t, \mathbf{k}), \\ \hat{\Psi}^R(t + \epsilon, \mathbf{k}) &= E_L^R(\epsilon\mathbf{k})\hat{\Psi}^L(t, \mathbf{k}) + E_R^R(\epsilon\mathbf{k})\hat{\Psi}^R(t, \mathbf{k}). \end{aligned} \tag{15}$$

For the three-step walk on the equilateral triangle lattice, the coefficients E read

$$\begin{aligned} E_L^L(\mathbf{q}) = {} & \sqrt{3}S[-1 - \exp(iq_x)\exp(-i\sqrt{3}q_y) + 3\exp(iq_x)\exp(+\sqrt{3}q_y) - \exp(2iq_x)] \\ & + C[-1 + 3\exp(iq_x)\exp(-i\sqrt{3}q_y) + 3\exp(iq_x)\exp(+i\sqrt{3}q_y) + 3\exp(2iq_x)], \end{aligned} \tag{16}$$

$$\begin{aligned} E_R^L(\mathbf{q}) = {} & iS[1 - 3\exp(-iq_x)\exp(-i\sqrt{3}q_y) + 3\exp(-iq_x)\exp(+i\sqrt{3}q_y) - 3\exp(-2iq_x)] \\ & + iC\sqrt{3}[-1 + 3\exp(-iq_x)\exp(-i\sqrt{3}q_y) - \exp(-iq_x)\exp(+i\sqrt{3}q_y) - \exp(-2iq_x)], \end{aligned} \tag{17}$$

$$\begin{aligned} E_L^R(\mathbf{q}) = {} & iS[1 - 3\exp(iq_x)\exp(-i\sqrt{3}q_y) - 3\exp(iq_x)\exp(+i\sqrt{3}q_y) - 3\exp(2iq_x)] \\ & + i\sqrt{3}C[-1 - \exp(iq_x)\exp(-i\sqrt{3}q_y) + 3i\exp(iq_x)\exp(+i\sqrt{3}q_y) - \exp(2iq_x)], \end{aligned} \tag{18}$$

$$\begin{aligned} E_R^R(\mathbf{q}) = {} & \sqrt{3}S[-1 + 3\exp(-iq_x)\exp(-i\sqrt{3}q_y) - \exp(-iq_x)\exp(+i\sqrt{3}q_y) - \exp(-2iq_x)] \\ & + C[-1 + 3\exp(-iq_x)\exp(-i\sqrt{3}q_y) + 3\exp(-iq_x)\exp(+i\sqrt{3}q_y) + 3\exp(-2iq_x)], \end{aligned} \tag{19}$$

where $C = \cos(3m\epsilon/2)/8$ and $S = \sin(3m\epsilon/2)/8$.

The first Brillouin zone of the equilateral triangle lattice is depicted in Fig. 1.

In Fourier space, linearly polarized plane waves $\Psi(t, \mathbf{X}) = A(\mathbf{k})\exp(i((\omega(\mathbf{k})t - \mathbf{k} \cdot \mathbf{X})))$ take of the form $\hat{\Psi}(t, \mathbf{k}) = A(\mathbf{k})\exp(i\omega(\mathbf{k})t)$. Inserting this *ansatz* into the equations of motion in Fourier space delivers, for each $\mathbf{k}$ in the Brillouin zone, a linear, homogeneous system obeyed by $A^L(\mathbf{k})$ and $A^R(\mathbf{k})$. For the three-step DQW on the equilateral triangle lattice, this system reads

$$\begin{aligned} F_L^L(\omega(\mathbf{k}), \mathbf{k})A^L(\mathbf{k}) + F_R^L(\mathbf{k})A^R(\mathbf{k}) = 0, \\ F_L^R(\mathbf{k})A^L(\mathbf{k}) + F_R^R(\omega(\mathbf{k}), \mathbf{k})A^R(\mathbf{k}) = 0, \end{aligned} \tag{20}$$

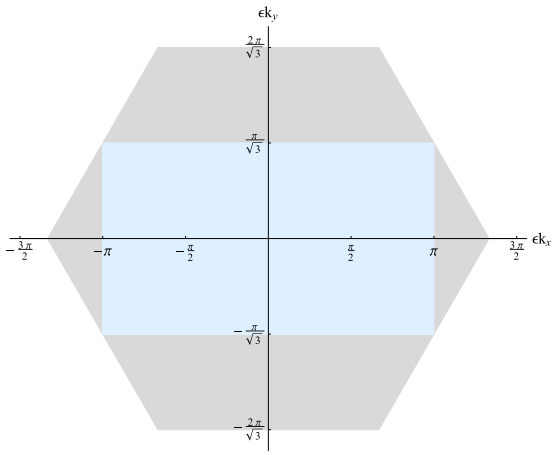

FIG. 1. First Brillouin zone of the equilateral triangle lattice (gray) and the periodicity domain of the three-step walk (light blue)

with $F_L^L(\omega(\mathbf{k}),\mathbf{k}) = \exp(i\omega(\mathbf{k})\epsilon) - E_L^L(\epsilon\mathbf{k})$, $F_R^R(\omega(\mathbf{k}),\mathbf{k}) = \exp(i\omega(\mathbf{k})\epsilon) - E_R^R(\epsilon\mathbf{k})$, $F_R^L(\mathbf{k}) = -E_R^L(\epsilon\mathbf{k})$, $F_L^R(\mathbf{k}) = -E_L^R(\epsilon\mathbf{k})$. This system has a nonvanishing solution $A(\mathbf{k})$ only if its determinant vanishes. Since the coefficients in this system are linear functions of $\Omega(\mathbf{k}) = \exp(i\omega(\mathbf{k})\epsilon)$, the determinant is a quadratic function of $\Omega(\mathbf{k})$. Equating this determinant to zero thus furnishes a quadratic equation for $\Omega(\mathbf{k})$, which can be solved exactly, delivering two solutions $\Omega_\pm(\mathbf{k})$ as functions of K_x and K_y. One thus obtains exact expressions $\pm\omega(\mathbf{k})$ for the two energy branches of each walk. These energies are exact opposite because the α angles of the free walks vanish identically, ensuring that the mixing operators are in $SU(2)$ and, thus, of unit determinant.

For each walk, the function $\omega(\mathbf{k})$ is periodic in $\mathbf{k}$ space, with the same periodicity domain as the coefficients F and E. For example, inspecting Eq. (19) reveals that $\omega(\mathbf{k})$ is peridiodic with periodicity domain $\mathcal{D}_\mathbf{k} = (-\pi,+\pi)\times(-\pi/\sqrt{3},+\pi/\sqrt{3})$ for the three-step walk on the equilateral triangle lattice. The periodicity domains of the other walks are $(-2\pi,+2\pi)\times(-2\pi/\sqrt{3},+2\pi/\sqrt{3})$ for the six-step walk, $(-\pi,+\pi)\times(-\pi,+\pi)$ for the isosceles lattice walk and $(-2\pi/3,+2\pi/3)\times(-2\pi/\sqrt{3},+2\pi/\sqrt{3})$ for the honeycomb lattice walk. These periodicity domains do *not* coincide with the Brillouin zones of the lattice. For example, Fig. 1 reveals that the periodicity domain of the three-step walk on the equilateral triangle lattice is smaller and entirely included in the Brillouin zone. This only means that some different wave vectors $\mathbf{k}$ are associated to the same frequency $\omega(\mathbf{k})$ (we recall that the waves under consideration do not describe vibrations of the lattice, but propagation of spin-1/2 fermions living on the lattice).

The dispersion relations are also periodic in the mass m, with period $4\pi/3$ for the two walks on the equilateral triangle lattice and 2π for the walk on the isosceles triangle lattice. The mass periodicity on the honeycomb lattice is $8\pi/3\sqrt{3}$.

The contours of the negative energy branch are plotted on $\mathcal{D}_\mathbf{k}$ in Figs. 2–5 for different values of the mass and for each of the four walks considered in this article respectively. Various conclusions can be drawn from the figures. First, one sees that, for each walk, varying the mass greatly influences the dispersion relation, changing for example the number and positions of the maxima and minima. As for the two walks defined on the equilateral triangle lattice, their symmetries are apparent on the dispersion relations, and both sets of contours therefore look very different (though both walks admit the same continuous limit). In particular, even the contours for vanishing mass are very different. The walk defined on the isosceles triangle lattice, whose continuous limit is also the flat space-time Dirac equation, gives rise to yet another set of

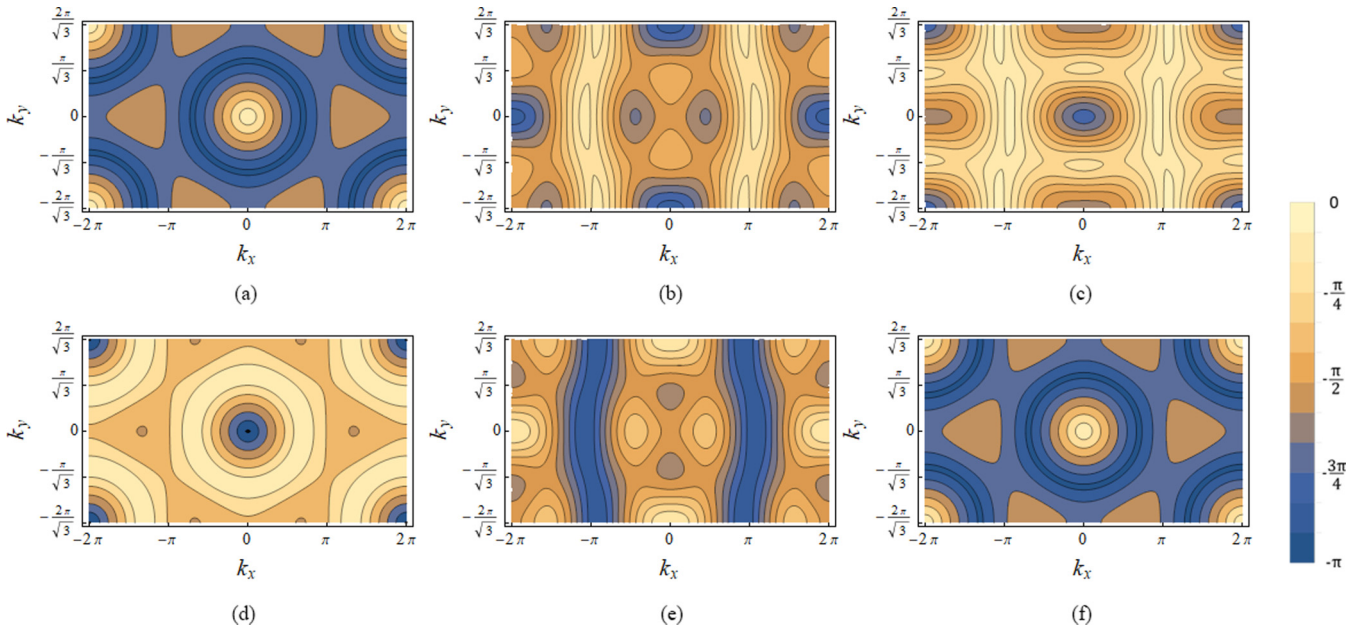

FIG. 2. Dispersion relations $\omega(\mathbf{k})$ for six-step DQW on the equilateral triangular lattice. (a) $m = 0$, (b) $m = \pi/3$, (c) $m = \pi/2$, (d) $m = 2\pi/3$, (e) $m = \pi$, (f) $m = 4\pi/3$.

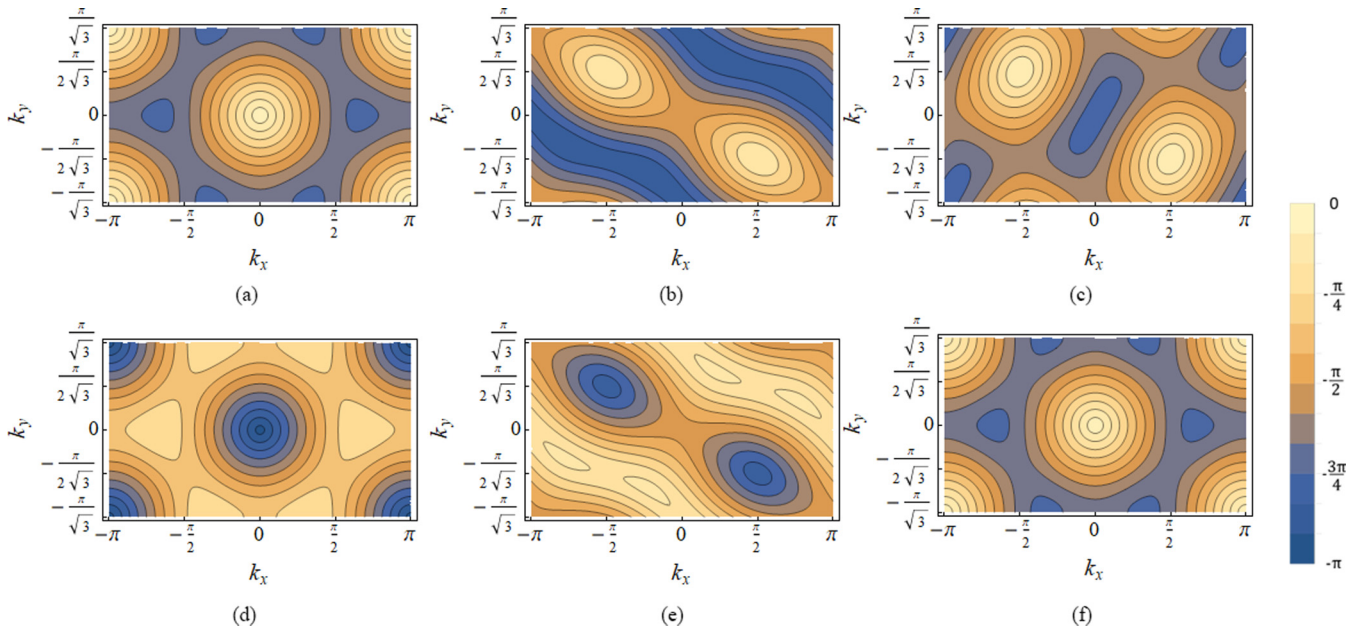

FIG. 3. Dispersion relations $\omega(\mathbf{k})$ for three-step DQW on the equilateral triangular lattice. (a) $m = 0$, (b) $m = \pi/3$, (c) $m = \pi/2$, (d) $m = 2\pi/3$, (e) $m = \pi$, (f) $m = 4\pi/3$.

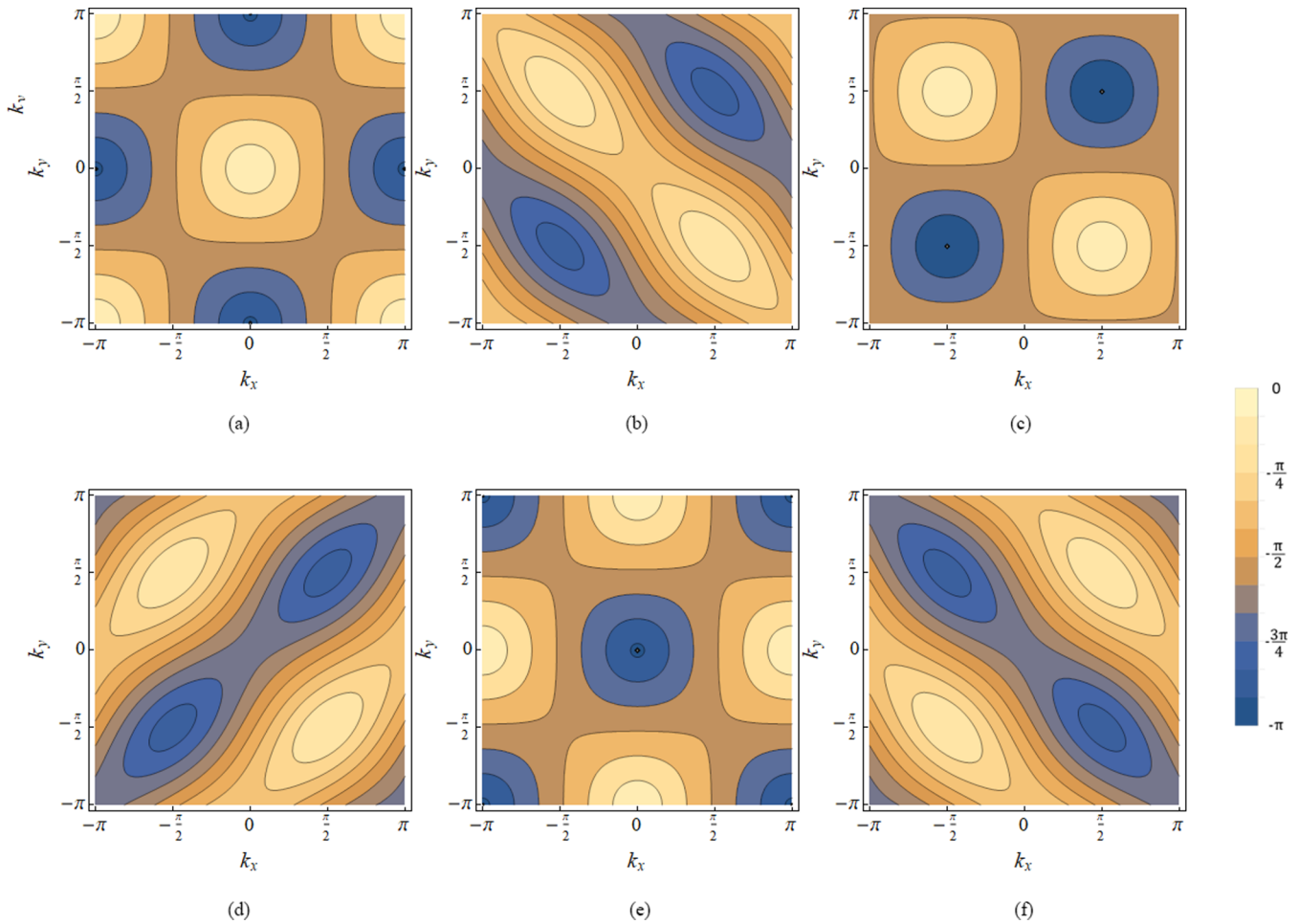

FIG. 4. Dispersion relations $\omega(\mathbf{k})$ for the DQW on the isosceles triangular lattice. (a) $m = 0$, (b) $m = \pi/3$, (c) $m = \pi/2$, (d) $m = 2\pi/3$, (e) $m = \pi$, (f) $m = 4\pi/3$.

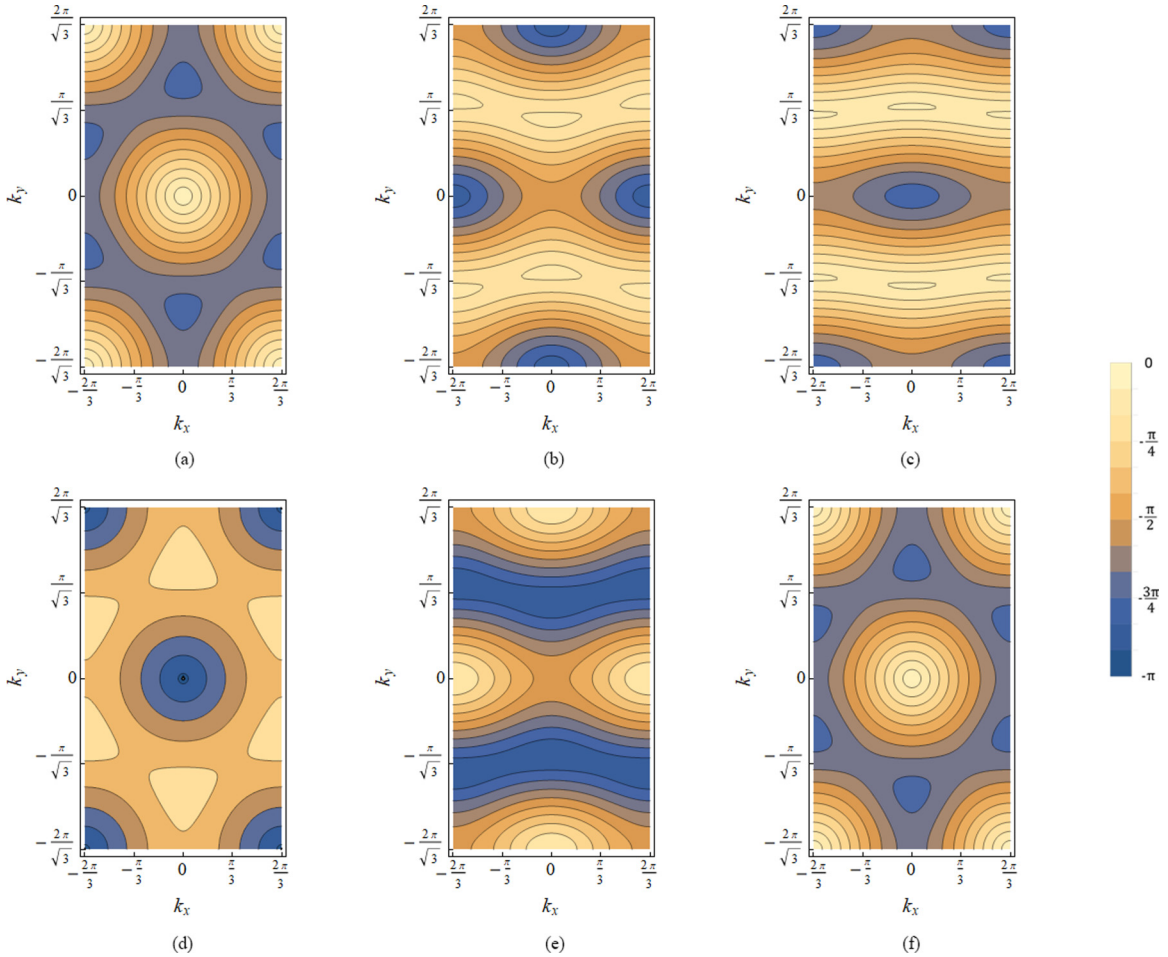

FIG. 5. Dispersion relations $\omega(\mathbf{k})$ for the DQW on the hexagonal honeycomb lattice. (a) $m = 0$, (b) $m = 2\pi/3\sqrt{3}$, (c) $m = \pi/\sqrt{3}$, (d) $m = 4\pi/3\sqrt{3}$, (e) $m = 2\pi/\sqrt{3}$, (f) $m = 8\pi/3\sqrt{3}$.

contours whose evolution with the mass m does not mirror the evolution obtained for the other two walks.

These contours have a direct consequence about the Zitterbewegung exhibited by the three walks. Let us recall that Zitterbewegung happens because of the interference of positive and negative energy solutions. For the Dirac equation, the two energy branches are $\omega_\pm = \pm\sqrt{\mathbf{k}^2 + m^2}$. Zitterbewegung thus happens at frequencies larger than the minimal energy gap $2m$, which is reached for $\mathbf{k} = 0$. Figs. 2–4 clearly show that, for nonvanishing values of m, the minimal energy gap of three walks considered in this article is inferior to $2m$ and is reached for nonvanishing values of the wave-vector $\mathbf{k}$. Thus, for nonvanishing mass, Zitterbewegung of frequency lower than $2m$ can be observed on wavepackets centered on nonvanishing values of $\mathbf{k}$. For vanishing mass, the six-step walk on the equilateral triangle lattice behaves exactly as solutions of the massless Dirac equation, i.e., there is no minimal frequency for Zitterbewegung, and the energy gap vanishes only at $\mathbf{k} = 0$. At vanishing mass, the other two walks exhibit a slightly different behavior. There is still a minimal frequency for Zitterbewegung, but the energy gap vanishes, not only at $\mathbf{k} = 0$, but also on the four corners of the periodicity domain. The minimal Zitterbewegung frequencies for the three triangular DQWs for various values of the mass are given in Tables I, II, and III.

IV. GAUGE-INVARIANT COUPLING TO ELECTROMAGNETIC FIELDS

A. Introducing the fields

The above DQWs are invariant by a global change of phase of the spinor Ψ, but they are not invariant under a local

TABLE I. Minimal frequencies for the equilateral triangle three-step DQW.

m	ω_m	$2\omega_m$	(k_x, k_y)
			(0,0)
0	0	0	$(\pm 3.14159, \pm 1.8138)$
			$(\pm 3.14159, \mp 1.8138)$
$\frac{\pi}{3}$	0.523599	1.0472	$(\pm 1.5708, \mp 0.9069)$
$\frac{\pi}{3}$	0.261799	0.523599	$(\pm 1.5708, \mp 0.9069)$
$\frac{2\pi}{3}$	1.76891	3.53783	$(\pm 1.0472, \pm 1.8138)$
			$(\pm 1.0472, \mp 1.8138)$
			$(\pm 2.0944, 0)$
π	0.446162	0.892324	$(\pm 0.701674, \pm 1.21534)$
			$(\pm 2.43992, \pm 0.598464)$
$\frac{4\pi}{3}$	0	0	(0,0)
			$(\pm 3.14159, \pm 1.8138)$
			$(\pm 3.14159, \mp 1.8138)$

TABLE II. Minimal frequencies for the equilateral triangle six-step DQW.

m	ω_m	$2\omega_m$	(k_x, k_y)
			(0,0)
0	0	0	$(\pm 6.28319, \pm 3.6276)$
			$(\pm 6.28319, \mp 3.6276)$
$\frac{\pi}{3}$	0.398927	0.797853	$(\pm 2.88854, \pm 3.6276)$
			$(\pm 2.88854, \mp 3.6276)$
			$(\pm 3.39465, 0)$
$\frac{\pi}{2}$	0.142285	0.284569	$(\pm 2.93021, 0)$
$\frac{2\pi}{3}$	0	0	$k_x^2 + k_y^2 = 2.20606^2$
			$(k_x \pm 6.283)^2 + (k_y \pm 3.628)^2 = 2.206^2$
			$(k_x \pm 6.283)^2 + (k_y \mp 3.628)^2 = 2.206^2$
π	0.523599	1.0472	$(\pm 6.28319, 0)$
			$(0, \pm 3.6276)$
$\frac{4\pi}{3}$	0	0	(0,0)
			$(\pm 6.28319, \pm 3.6276)$
			$(\pm 6.28319, \mp 3.6276)$

change of phase. However, they can all be transformed into locally $U(1)$ gauge-invariant walks. We will now present in detail the principle behind this generalization on the three-step DQW defined on the equilateral triangle lattice. Adding an electromagnetic field to the other three walks can be done in a similar way.

To achieve local $U(1)$ gauge invariance, we define each U_i operator entering the definition of the walk by

$$(U_i\Psi)(t, \mathbf{X}) = U(\alpha_i(t, \mathbf{X}), \xi_i(t, \mathbf{X}), \zeta_i(t, \mathbf{X}), 0)\Psi(t, \mathbf{X}), \tag{21}$$

where the α_i's, ξ_i's, and ζ_i's are arbitrary functions of t and $\mathbf{X}$. Note that the choice $\theta_i = 0$ make the walk actually independent of ζ_i.

Let us break down the definition of the walk in three time substeps and write

$$\begin{aligned}\Psi(t + \Delta t/3) &= U_1(t)\tilde{S}_1\Psi(t),\\ \Psi(t + 2\Delta t/3) &= \tilde{R}_1^{-1}U_2(t)\tilde{S}_2\tilde{R}_1\Psi(t + \Delta t/3),\\ \Psi(t + \Delta t) &= \tilde{R}_2^{-1}U_3(t)\tilde{S}_3\tilde{R}_2\Psi(t + 2\Delta t/3).\end{aligned} \tag{22}$$

Let ϕ be the phase of the spinor Ψ and consider an arbitrary local change of phase $\phi'(t + r\Delta t/3, \mathbf{X}) = \phi(t + r\Delta t/3, \mathbf{X}) + \delta\phi(t + r\Delta t/3, \mathbf{X})$ for all $(t, \mathbf{X})$ and $r = 0, 1, 2$. Note that one thus allows for an arbitrary change of phase, not only at all integer time steps, but also at all intermediate time substeps. We accompany this arbitrary change of phase by a change in the functions α_i, ξ_i, and ζ_i, introducing $\alpha_i'(t, \mathbf{X}) = \alpha_i(t, \mathbf{X}) + \delta\alpha_i(t, \mathbf{X})$ and so on.

TABLE III. Minimal frequencies for the isosceles triangle DQW.

m	ω_m	$2\omega_m$	(k_x, k_y)
			(0,0)
0	0	0	$(\pm 3.14159, \pm 3.14159)$
			$(\pm 3.14159, \mp 3.14159)$
$\frac{\pi}{3}$	0.523599	1.0472	$(\pm 1.5708, \mp 1.5708)$
$\frac{\pi}{2}$	0	0	$(\pm 1.5708, \mp 1.5708)$
$\frac{2\pi}{3}$	0.523599	1.0472	$(\pm 1.5708, \mp 1.5708)$
π	0	0	$(\pm 3.14159, 0)$
			$(0, \pm 3.14159)$
$\frac{4\pi}{3}$	0.523599	1.0472	$(\pm 1.5708, \pm 1.5708)$

Focus now on the first intermediate evolution equation between time t and time $t + \Delta t/3$. A direct computation identical to the one already presented for DQWs in two-dimensional space-times reveals that this equation is identical for the primed and the unprimed walk provided

$$\begin{aligned}\delta\alpha_1(t, \mathbf{X}) &= \delta\phi(t + \Delta t/3, \mathbf{X}) - \sigma_1(t, \mathbf{X}),\\ \delta\xi_1(t, \mathbf{X}) &= -\delta_1(t, \mathbf{X}),\end{aligned} \tag{23}$$

where $\sigma_1(t, \mathbf{X}) = (\delta\phi(t, \mathbf{X}_1) + \delta\phi(t, \mathbf{X}_4))/2$ and $\delta_1(t, \mathbf{X}) = (\delta\phi(t, \mathbf{X}_1) - \delta\phi(t, \mathbf{X}_4))/2$. There is no constraint on ζ_i' because it actually does not enter the definition of the walk.

Let us now proceed to the second time substep. It seems like the situation is more complex but it is actually identical because a local change of phase affects both components of the spinor identically and, thus, commute with the operator R_1. One thus obtains local gauge invariance at this time substep if

$$\begin{aligned}\delta\alpha_2(t, \mathbf{X}) &= \delta\phi(t + 2\Delta t/3, \mathbf{X}) - \sigma_2(t, \mathbf{X}),\\ \delta\xi_2(t, \mathbf{X}) &= -\delta_2(t, \mathbf{X}),\end{aligned} \tag{24}$$

where $\sigma_2(t, \mathbf{X}) = (\delta\phi(t + \Delta t/3, \mathbf{X}_2) + \delta\phi(t + \Delta t/3, \mathbf{X}_5))/2$ and $\delta_2(t, \mathbf{X}) = (\delta\phi(t + \Delta t/3, \mathbf{X}_2) - \delta\phi(t + \Delta t/3, \mathbf{X}_5))/2$. The same reasoning goes for the third and final time substep and gauge invariance at this substep is provided if

$$\begin{aligned}\delta\alpha_3(t, \mathbf{X}) &= \delta\phi(t + \Delta t, \mathbf{X}) - \sigma_3(t, \mathbf{X}),\\ \delta\xi_3(t, \mathbf{X}) &= -\delta_3(t, \mathbf{X}),\end{aligned} \tag{25}$$

where $\sigma_3(t, \mathbf{X}) = (\delta\phi(t + 2\Delta t/3, \mathbf{X}_3) + \delta\phi(t+2\Delta t/3, \mathbf{X}_6))/2$ and $\delta_3(t, \mathbf{X}) = (\delta\phi(t + 2\Delta t/3, \mathbf{X}_3) - \delta\phi(t + 2\Delta t/3, \mathbf{X}_6)/2$.

One way to acknowledge that substeps are just substeps, and not full time-steps, is to consider phase changes such that $\delta\phi(t, \mathbf{X}) = \delta\phi(t + \Delta t/3, \mathbf{X}) = \delta\phi(t + 2\Delta t/3, \mathbf{X})$ (compare in particular with the definition of the α_i's, ξ_i's, and ζ_i's, which are indexed by t, though all describe what happens between intermediate substeps). For these phase changes, the above equations simplify into

$$\begin{aligned}\delta\alpha_3(t, \mathbf{X}) &= \delta\phi(t + \Delta t, \mathbf{X}) - \sigma_3(t, \mathbf{X}),\\ \delta\alpha_2(t, \mathbf{X}) &= \delta\phi(t, \mathbf{X}) - \sigma_2(t, \mathbf{X}),\\ \delta\alpha_1(t, \mathbf{X}) &= \delta\phi(t, \mathbf{X}) - \sigma_1(t, \mathbf{X}),\\ \delta\xi_i(t, \mathbf{X}) &= -\delta_i(t, \mathbf{X}),\end{aligned} \tag{26}$$

where $\sigma_i(t, \mathbf{X}) = (\delta\phi(t, \mathbf{X}_i) + \delta\phi(t, \mathbf{X}_{i+3}))/2$, $\delta_i(t, \mathbf{X}) = (\delta\phi(t, \mathbf{X}_i) - \delta\phi(t, \mathbf{X}_{i+3}))/2$ for $i = 1, 2, 3$.

Another natural classes of phase changes is defined by the relations

$$\begin{aligned}&\delta\phi(t + \Delta t/3, \mathbf{X}) - \delta\phi(t, \mathbf{X})\\ &\qquad = \tfrac{1}{3}(\delta\phi(t + \Delta t, \mathbf{X}) - \delta\phi(t, \mathbf{X})),\\ &\delta\phi(t + 2\Delta t/3, \mathbf{X}) - \delta\phi(t + \Delta t/3, \mathbf{X})\\ &\qquad = \tfrac{1}{3}(\delta\phi(t + \Delta t, \mathbf{X}) - \delta\phi(t, \mathbf{X})).\end{aligned} \tag{27}$$

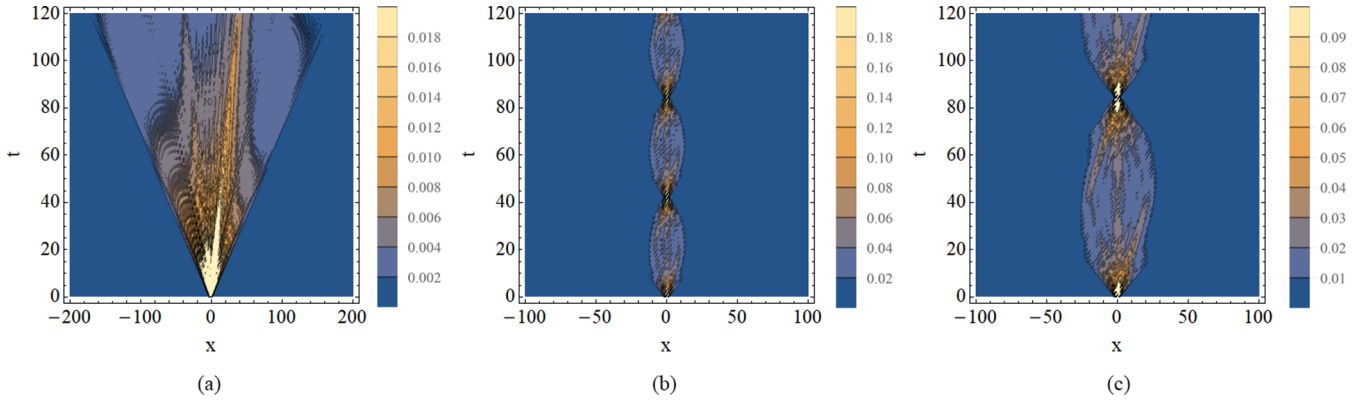

FIG. 6. Density plots in (t, x) of (a) no electric field (free space), and (b, c) electric field in the x direction with $E_x = 0.1$ and $E_x = 0.05$, respectively.

For these phase changes, the gauge transformation of the α_i's and ξ_i's simplifies into

$$\begin{aligned} \delta\alpha_i(t, \mathbf{X}) &= -\tfrac{1}{3}(\delta\phi(t, \mathbf{X})) - \sigma_i(t, \mathbf{X}), \\ \delta\xi_i(t, \mathbf{X}) &= -\delta_i(t, \mathbf{X}), \end{aligned} \tag{28}$$

for $i = 1, 2, 3$.

To perform the continuous limit, we write $\alpha_i = \epsilon\bar{\alpha}_i$, $\xi_i = \epsilon\bar{\xi}_i$, $\zeta_i = \epsilon\bar{\zeta}_i$, and let ϵ tend to zero, keeping all bar angles finite. The DQW dynamics then delivers the Dirac equation with electromagnetic potential

$$\begin{aligned} A_0 &= \frac{2}{3}(\bar{\alpha}_1 + \bar{\alpha}_2 + \bar{\alpha}_3), \\ A_1 &= -\frac{2}{3}\left(\bar{\xi}_1 + \frac{1}{2}(\bar{\xi}_2 - \bar{\xi}_3)\right), \\ A_2 &= -\frac{1}{\sqrt{3}}(\bar{\xi}_2 + \bar{\xi}_3). \end{aligned} \tag{29}$$

B. Motion in a uniform constant electric field

Based on the above relations between (A_0, A_1, A_2) and the phase variables α_i and ξ_i a simple way to couple the DQW to a constant homogeneous electric field of Cartesian components E_1 and E_2 is to choose identically vanishing α_i's and to impose $\xi_1 = 0$ together with

$$\begin{aligned} \xi_2 &= \tfrac{1}{2}(-3E_x + \sqrt{3}E_y), \\ \xi_3 &= \tfrac{1}{2}(+3E_x + \sqrt{3}E_y). \end{aligned} \tag{30}$$

Consider first the case $E_y = 0$. Figures 6 and 7 presents contour plots of the walk projected unto the (t, x) and (t, y) planes for various values of E_x and for the symmetric initial condition $\Psi = (1/\sqrt{2}, 1/\sqrt{2})^\top$. Note that this initial condition probes the walk dynamics outside the continuous limit. This point will be discussed in the final section.

In the presence of a nonvanishing electric field, the spreading characteristic of the free walk is replaced by apparent oscillations with identical periods in the x and in the y directions. These oscillations can be understood qualitatively by recalling that, in one spatial dimension, a quantum particle moving in continuous space-time submitted to the action of a uniform homogeneous electric field E combined with a periodic potential undergo oscillations [35]. The period T_B of these oscillations is called the Bloch period and $T_B = 2\pi/E$ as the periodicity domain is of length 2π. Without getting into detailed computations, the periodicity of the potential generates a finite-sized periodicity domain in momentum space and the period of the oscillations correspond to the time

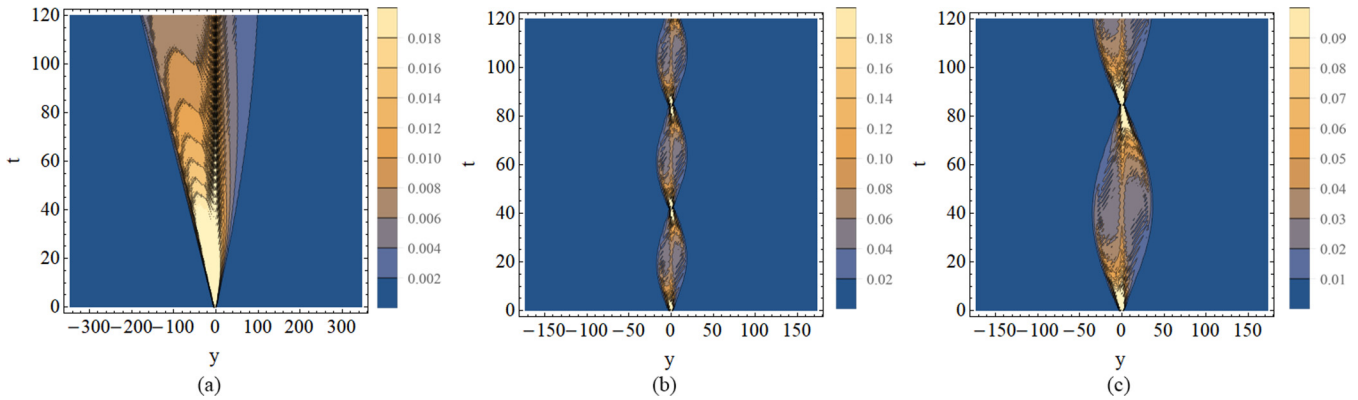

FIG. 7. Density plots in (t, y) of (a) no electric field (free space), and (b), (c) electric field in the x direction with $E_x = 0.1$ and $E_x = 0.05$, respectively.

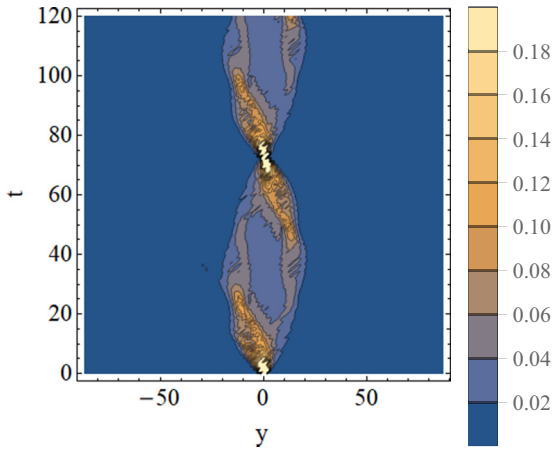

FIG. 8. Density plot of electric field in the y direction: $E_y = 0.1$

necessary for the particle to cross this periodicity domain in momentum space. In the case presented in Fig. 6, there is evidently no periodic potential, but the quantum walk does admit a finite-sized periodicity domain of length 2π along the x axis. The apparent period coincides exactly with the Bloch period, if one takes into account the $3/2$ proportionality factor between the time t used to parametrize the walk and the standard choice of continuous time in the Dirac equation (see above).

This interpretation of the observed oscillations can be confirmed by two numerical experiments. First choose now an electric field in the y direction. The length of the periodicity domain in the y direction is $2\pi/\sqrt{3}$, so the Bloch period is now $T_B^y = T_B/\sqrt{3}$. Oscillations at this period are indeed observed on Fig. 8. Choose now an electric field with equal components in the x and y directions. Since the lengths of the x direction and y direction of the periodicity domain differs by a multiplicative factor of $\sqrt{3}$, their ratio is not a rational number and there is no reason to expect any periodicity in the walk. This is indeed displayed in Fig. 9, which is obtained for $\mathbf{E} = (1, 1)$.

V. CONCLUSION

We propose four different DQWs on two regular triangular lattices and one hexagonal honeycomb lattice, and prove that they all admit the free Dirac equation as continuous limits. We analyze in depth the qualitative difference between the four walks, and their consequences for Zitterbewegung. We also show that these walks can be extended to incorporate a gauge-invariant coupling to discrete electromagnetic fields and addressed Bloch-like oscillations. These results show that DQWs defined on more general lattices than the square lattice can be used to study the free Dirac dynamics and that coupling the walks to arbitrary electromagnetic fields in a gauge-invariant manner is also possible.

Let us comment briefly on some of these results before mentioning avenues left open for further study. Until now, DQW admitting the Dirac equation as continuous limit had only been defined on spatial regular square lattices embedded in flat Euclidean space. At each point of these lattices, the number of edges is exactly twice the space dimension, and the construction of the DQWs is therefore quite natural: one first translates and mixes along the two edges corresponding to the x-direction, and then along the two edges corresponding the to y-dimension. Consider now a triangular lattice embedded in flat two-dimensional (2D) Euclidean space. For each point, the number of edges is three times the space dimension. If one wants to obtain a DQW that admits the Dirac equation as continuous limit, one must use two component spinors only, and find a way to translate and mix along all six edges in a manner which, at the continuous limit, appears isotropic, not forgetting that at least four edges are not parallel to the x or the y direction. This is precisely what is done in the article. What is perhaps more interesting is that (i) this can be done in at least two different ways on the equilateral triangle lattice (ii) this *de facto* gives rise to DQWs on the honeycomb lattice (iii) all DQWs can be coupled to EM fields in a gauge-invariant manner. Point (iii) is especially nontrivial because the exact discrete gauge invariance involves finite differences along the three edge directions while the standard continuous change of gauge relations involve gradients along the two Cartesian spatial dimensions.

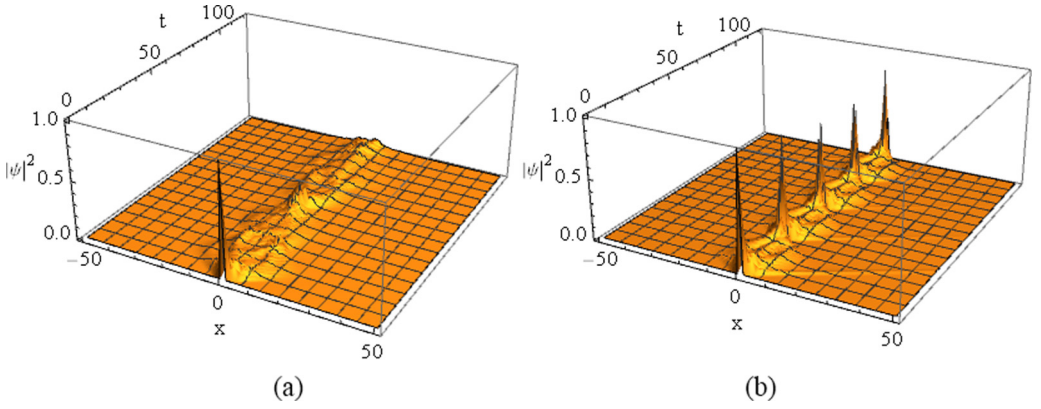

FIG. 9. Density plots of (a) electric field in both the x-direction and y-direction: $E_x = 0.1$ and $E_y = 0.1$, and (b) electric field only in the x direction of equivalent magnitude ($E_x = \frac{\sqrt{2}}{10}$)

A comment on the use of BZs and periodicity domains is in order. Given an arbitrary lattice L, any function defined in L can be expanded in a unique way in exponential functions with wave vectors $\mathbf{k}$ in the Brilllouin zone B_L of the lattice L. This is the discrete Fourier decomposition adopted in this article. If one now considers a d-component object Ψ, its discrete Fourier transform has also d components. Suppose Ψ obeys a certain dynamics $\mathcal{D}$ on L, one can search for eigenmodes of this dynamics and one obtains d branches or bands, each one defined on the full Brillouin zone B_L of the lattice L. In this article, $d = 2$ and the two energy branches are symmetric with respect to the $\mathbf{k}$ plane (one positive, the other negative). Now, it may happen that the dynamics $\mathcal{D}$ one studies on L makes it interesting to split L into several sublattices L_1, L_2, and so on. For example, the usual discrete dynamics modeling transport in graphene [36] couples only close neighbors and this makes it natural to partition the full graphene honeycomb lattice into two sublattice lattices L_1 and L_2. Each of these sublattices is associated to the same reduced Brillouin zone $B_{L_1} = B_{L_2} = \bar{B}$ which is twice as small as the Brillouin zone B_L of the original true graphene lattice. By definition, defining *one* function on L is identical to defining *one* function on L_1 and *one* function on L_2. Fourier-transforming these two functions delivers *two* functions defined on the reduced Brillouin zone $\bar{B}$ (which makes sense because $\bar{B}$ is twice as small as B_L). Thus, a single, zero spin wave function defined on the full lattice L can be converted into two zero-spin wave functions, each defined on one of the sublattices, which in turn get converted into two functions defined on the common reduced Brillouin zone $\bar{B}$, which are then identified, for small wave vectors $\mathbf{k}$ with the two components of a 2D Dirac spinor. Thus, the usual transport model in graphene can be studied by two alternative methods which, naturally deliver the same results. The first method deals with a single, one-component wave function defined on the full graphene lattice L or, alternately, its one-component discrete Fourier transform defined on the full BZ B_L. The second method deals with two one-component wave functions, each defined on one sublattice, which are ultimately converted into a two-component wave function defined on the reduced Brillouin zone $\bar{B}$. Both methods deliver the same (number of) eigenmodes, but encoded in a different way. If one uses the first method, a single eigenmode corresponds to each wavevector in the full BZ B_L. If one uses the second method, two eigenmodes correspond to each wavevector in the reduced BZ $\bar{B}$. But the reduced BZ $\bar{B}$ is twice as small as the true BZ B_L and one thus recovers the same (number of) modes.

Though this procedure delivers a useful and interesting interpretation of the usual transport model in graphene, it relies on the natural splitting of the original lattice into sublattices induced by the dynamics $\mathcal{D}$ describing the transport. Thus, the splitting is not intrinsic to the lattice L one considers, but depends on both the lattice L and the dynamics $\mathcal{D}$. This is why this procedure has not been retained in the present article. Indeed, among the four QWs considered in this article, two of them involve different dynamics defined on the same lattice. The only meaningful way to compare these two QWs is to work with what is intrinsic to the lattice on which they are defined, i.e., to work on the full BZ of this lattice.

Finally, for all QWs considered here, a full time-step involves several subtime steps. Each subtime step couples close neighbors but breaks the symmetry of the lattice, which is, however, restored at the level of the full time-step. This construction is actually necessary to bypass the "no-go" theorem presented in Refs. [37,38] and define the DQWs on the lattice considered in this article. Since each subtime step only couples close neighbors on the lattice, it follows that a full-time step does *not* couple close neighbors, but points whose separation is *larger* than the distance between close neighbours. Therefore, the periodicity domains of the eigenmodes are *smaller* than the full BZ B_L. Thus, one works in the full BZ B_L, the modes are labeled by an arbitrary $\mathbf{k} \in B_L$, different $\mathbf{k}$'s in B_L correspond to different modes, but some modes, though distinct because labeled by different $\mathbf{k}'s$, have the same frequencies ω.

The initial condition used in the numerical simulations of Sec. IV B probes the walk outside the continuous limit. The result of these simulations, i.e., oscillations at the Bloch frequency proves that concepts and results derived from the continuous limit can be useful in analyzing the walk well within the discrete regime. The fact that the discrete regime of DQWs may exhibit aspects qualitatively similar to the continuous regime has already been pointed out on other DQWs [20].

Many interesting questions still remain open. The first class of extensions addresses questions on triangular lattices. For example, what continuous limit does one obtain if one embeds a triangle lattice in Euclidean space of dimension higher than two? Or, can one incorporate other Yang-Mills fields and gravity on triangular lattices? And can one define gauge-invariant field strengths for the Yang-Mills fields and gravity? Also, what about irregular triangular lattices, for example with defects?

The second set of questions addresses other lattices and more general discrete structures. Can the results presented in this work be extended to arbitrary regular and nonregular lattices on the 2D plane and in spaces of higher dimensions? Do they also translate on graphs, at least regular ones? And can one couple DQWs on graphs with Yang-Mills fields and gravity? Such questions will be addressed in our future work.

ACKNOWLEDGMENTS

GJ and JBW would like to thank Ian McArthur for useful discussions on quantum walks and Dirac dynamics in general.

Note added. Another team from France and Spain worked independently on DQWs [39] on nonsquare lattices and we exchanged our manuscripts [40] after both were completed. The other team offered a very clear and constructive presentation of two DQWs built out of identical substeps.

[1] R. P. Feynman and A. R. Hibbs, *Quantum Mechanics and Path Integrals* (McGraw-Hill, New York, 1965).

[2] S. S. Schweber, Rev. Mod. Phys. **58**, 449 (1986).

[3] Y. Aharonov, L. Davidovich, and N. Zagury, Phys. Rev. A **48**, 1687 (1993).

[4] D. A. Meyer, J. Stat. Phys. **85**, 551 (1996).

[5] A. Ambainis, SIAM J. Comput. **37**, 210 (2007).
[6] F. Magniez, A. Nayak, J. Roland, and M. Santha, SIAM J. Comput. **40**, 142 (2011).
[7] K. Manouchehri and J. B. Wang, *Physical Implementation of Quantum Walks* (Springer, New York, 2014).
[8] F. W. Strauch, Phys. Rev. A **73**, 054302 (2006).
[9] F. Strauch, J. Math. Phys. **48**, 082102 (2007).
[10] P. Kurzynski, Phys. Lett. A **372**, 6125 (2008).
[11] C. M. Chandrashekar, Sci. Rep. **3**, 2829 (2013).
[12] Y. Shikano, J. Comput. Theor. Nanosci. **10**, 1558 (2013).
[13] P. Arrighi, V. Nesme, and M. Forets, J. Phys. A: Math. Theor. **47**, 465302 (2014).
[14] P. Arrighi, S. Facchini, and M. Forets, Quant. Info. Proc. **15**, 3467 (2016).
[15] G. D. Molfetta, L. Honter, B. Luo, T. Wada, and Y. Shikano, Quantum Stud.: Math. Found. **2**, 243 (2015).
[16] A. Pérez, Phys. Rev. A **93**, 012328 (2016).
[17] A. Bisio, G. M. D'Ariano, and P. Perinotti, Phys. Rev. A **94**, 042120 (2016).
[18] G. Di Molfetta, M. Brachet, and F. Debbasch, Phys. Rev. A **88**, 042301 (2013).
[19] G. Di Molfetta, M. Brachet, and F. Debbasch, Physica A **397**, 157 (2014).
[20] P. Arnault and F. Debbasch, Physica A **443**, 179 (2016).
[21] P. Arnault and F. Debbasch, Phys. Rev. A **93**, 052301 (2016).
[22] P. Arnault, G. Di Molfetta, M. Brachet, and F. Debbasch, Phys. Rev. A **94**, 012335 (2016).
[23] P. Arnault and F. Debbasch, Ann. Phys. (NY) **383**, 645 (2017).
[24] A. Bisio, G. M. D'Ariano, and A. Tosini, Ann. Phys. (NY) **354**, 244 (2015).
[25] I. Márquez, P. Arnault, G. Di Molfetta, and A. Pérez, Phys. Rev. A **98**, 032333 (2018).
[26] I. Bialynicki-Birula, Phys. Rev. D **49**, 6920 (1994).
[27] E. R. G. Valcarcel and A. Romanelli, New J. Phys. **12**, 123022 (2010).
[28] A. Ahlbrecht, H. Vogts, A. H. Werner, and R. F. Werner, J. Math. Phys. **52**, 042201 (2011).
[29] M. Hinarejos, A. Peez, E. Roldán, A. Romanelli, and G. Valcarcel, New J. Phys. **15**, 073041 (2013).
[30] J. Schliemann, D. Loss, and R. M. Westervelt, Phys. Rev. Lett. **94**, 206801 (2005).
[31] R. Gerritsma, G. Kirchmair, F. Zaringer, E. Solano, R. Blatt, and C. F. Roos, Nature **463**, 68 (2010).
[32] A. Bisio, G. M. D'Ariano, and A. Tosini, Phys. Rev. A **88**, 032301 (2013).
[33] F. Bloch, Z. Phys. **52**, 555 (1929).
[34] D. Tamascelli, S. Olivares, R. O. S. Rossotti, and M. G. A. Paris, Sci. Rep **6**, 26054 (2016).
[35] T. Hartmann, F. Keck, H. Korsch, and S. Mossmann, New J. Phys. **6**, 2 (2004).
[36] M. I. Katsnelson, *Graphene: Carbon in Two Dimensions* (Cambridge University Press, Cambridge, England, 2012).
[37] G. M. D'Ariano and P. Perinotti, Phys. Rev. A **90**, 062106 (2014).
[38] G. M. D'Ariano, M. Erba, and P. Perinotti, Phys. Rev. A **96**, 062101 (2017).
[39] P. Arrighi, G. Di Molfetta, I. Márquez-Martín, and A. Pérez, Phys. Rev. A **97**, 062111 (2018).
[40] G. Jay, F. Debbasch, and J. B. Wang, arXiv:1803.01304, 2018.